



## Brief communication: Measuring and modelling the ice thickness of the Grigoriev ice cap (Kyrgyzstan) and comparison with global datasets.

Lander VAN TRICHT<sup>1</sup>, Chloë Marie PAICE<sup>1</sup>, Oleg RYBAK<sup>1,2,3</sup>, Philippe HUYBRECHTS<sup>1</sup>

5 <sup>1</sup>Earth System Science & Departement Geografie, Vrije Universiteit Brussel, Pleinlaan 2, B-1050 Brussels, Belgium

<sup>2</sup>Water Problems Institute, Russian Academy of Sciences, ul. Gubkina 3, Moscow, 119333 Russia

<sup>3</sup>FRC SSC RAS, ul. Ya. Fabritsiusa 2/28, Sochi, 354002 Russia

\*Corresponding author: Lander Van Tricht ([lander.van.tricht@vub.be](mailto:lander.van.tricht@vub.be))

10

**Abstract.** An accurate ice thickness distribution is crucial for correct projections of the future state of an ice mass. However, measuring the ice thickness with an in-situ system is time-consuming and not scalable. Therefore, models have been developed that estimate the ice thickness without direct measurements. In this study, we reconstruct the ice thickness of the Grigoriev ice cap, Kyrgyzstan, from in-situ observations and the yield stress method. We compare the results with data from 6 global ice thickness datasets composed without the use of our local measurements. The results highlight shortcomings of these generic datasets and demonstrate the importance of local observations for accurate representations of the ice thickness.

15

### 1. Introduction

20

The ice thickness distribution is an essential element in glaciological modelling studies as it represents the initial conditions of a glacier or ice cap in a model (Farinotti et al., 2017). To make projections about future evolution and runoff, a correct representation of ice thickness and volume is thus essential. Because ice thickness field campaigns are often dangerous, time-consuming, and not scalable to all glaciers, detailed thickness data or distributions based on in situ measurements (e.g. radio-echo soundings), have only been obtained on just over a thousand glaciers and ice caps of the >200,000 remaining worldwide (Clarke et al., 2009; Welty et al., 2020). The aim of this brief communication is to present our measurements and reconstructed ice thickness distribution of the Grigoriev ice cap. During our multi-day field campaign in 2021, we measured the ice thickness at > 500 points using Radio Echo Sounding (RES). These radar measurements were converted into ice thickness and subsequently interpolated to the entire ice cap using an approach based on the yield stress. Next to that, we compare the obtained ice thickness field with the results from six global datasets composed without the use of our in-situ measurements (Farinotti et al., 2019; Millan et al., 2022).

25

30

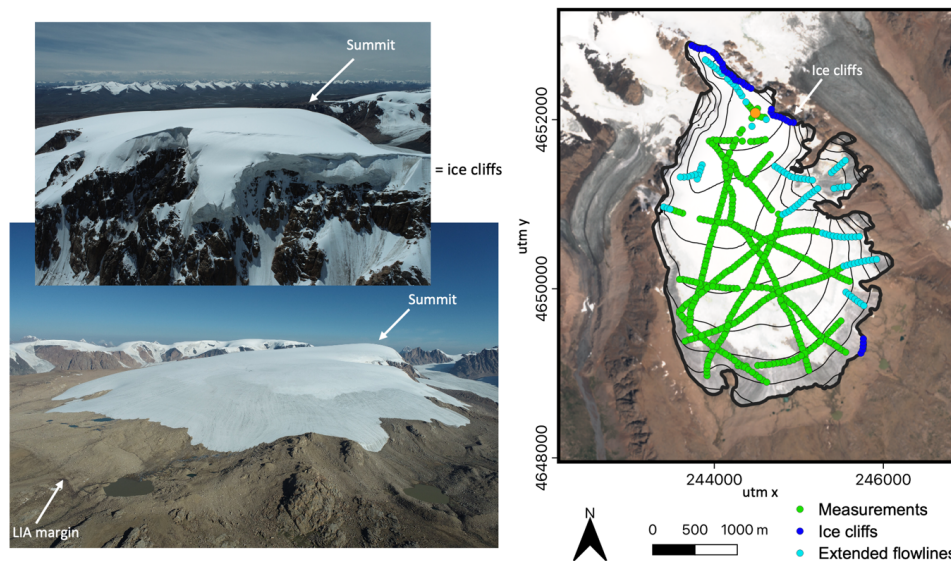
### 2. Grigoriev ice cap

35

The Grigoriev ice cap (Figure 1) is located in the Inner Tien Shan (Kyrgyzstan, Central Asia) on the southern slopes of the Terskey Ala-Too mountain range, about 30 km northeast of the Kumtor Gold Mine and the Ak-Shyirak massif. The almost circular ice cap, which is also called “a flat top glacier”, has an altitude between 4200 and 4600 m a.s.l. It is subject to a cold continental climate with a limited amount of precipitation, as the area is surrounded by high mountain ranges which protect the glaciers from incoming moisture. At the Kumtor-Tien Shan weather station (3659 m a.s.l.), the total annual precipitation is only 350 mm (Van Tricht et al., 2021). Most of the precipitation falls in spring and summer (75%), primarily as a result of convection. In winter, the Siberian High with accompanying dry conditions rules over the region. The Grigoriev ice cap is thus an example of a spring/summer accumulation type of ice cap. In the past, several glaciological measurements were performed on the ice cap, ranging from ice temperature measurements (Dikikh, 1965; Thompson et al., 1993; Arkhipov et al., 2004; Takeuchi et al., 2014) to surface mass balance measurements (Mikhaleiko, 1989; Dyurgerov, 2002; Arkhipov et al., 2004; Fujita et al., 2011). According to the modelling study by Van Tricht and Huybrechts (2022), the ice cap has a cold thermal regime.

40

45



50

**Figure 1:** (left) View over the Grigoriev ice cap and the ice cliffs in August 2021. Both images are made with a DJI Phantom 4 RTK. (right) Grigoriev ice cap in August 2021. The background is from Sentinel-2 in July 2021. The elevation contours are drawn for every 50 m, starting from 4200 m a.s.l. The black outline of the ice cap is from August 2021. The coordinate system corresponds to the EPSG:32644 WGS 84 / UTM zone 44N.

55

### 3. Measurements and modelling

#### 3.1. Ice thickness measurements and drone data

60

The use of a radar or RES system to derive the ice thickness is based on the difference in permeability between ice and the underlying bedrock. As an electromagnetic wave travels more easily through ice than through bedrock, it will be reflected by the bedrock. Based on the difference in travel time between the reflected wave and the direct wave through the air, the ice thickness can be inferred (Figure 2) (Eq. 1):

$$H = \frac{1}{2} * \left[ v_{ice}^2 \left( \Delta t + \frac{d}{v_{air}} \right)^2 - d^2 \right]^{\frac{1}{2}} \quad (1)$$

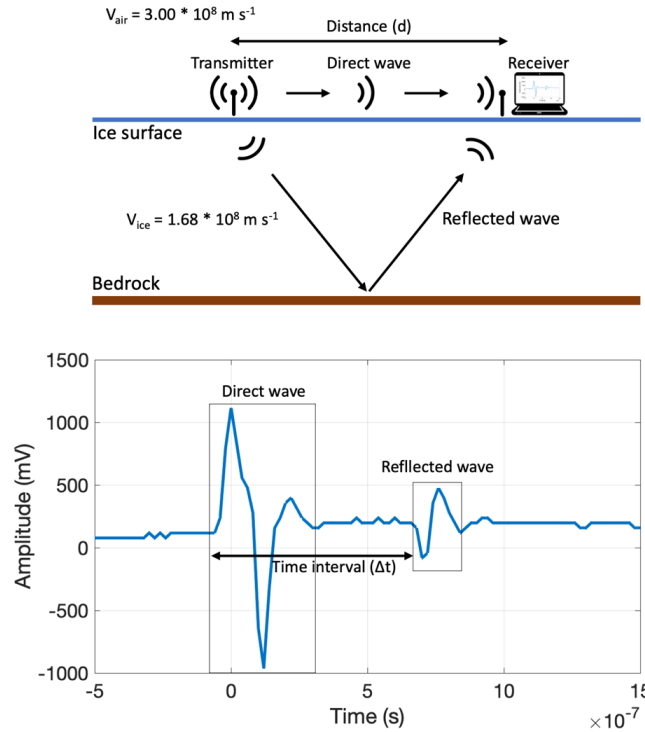
65

with  $v_{ice}$  the velocity of the wave through ice, assumed to be  $1.68 \times 10^8 \text{ m s}^{-1}$ , and  $v_{air}$  the velocity of the wave through air, equal to  $3.00 \times 10^8 \text{ m s}^{-1}$ .  $H$  is the ice thickness,  $\Delta t$  the time difference between the reception of both waves, and  $d$  is the physical distance between the transmitter of the wave and the receiver (typically 30-40 m).

70

In August 2021, we performed a multi-day field campaign on the Grigoriev ice cap to measure the ice thickness at more than 500 locations with a handheld ground penetrating radar (Narod and Clarke, 1994) (Figure 1). Following the setup of previous field campaigns (Van Tricht et al., 2021a), a radio signal with a frequency of 5 MHz was chosen. The uncertainty of the ice thickness measurements is estimated to be  $8 \text{ m} \pm 5\%$ . In addition to the radar measurements, a DJI Phantom 4 RTK drone was used to capture > 1000 images to reconstruct the surface elevation of the ice cap in Pix4D (Van Tricht et al. 2021c). GPS measurements of the locations of the transmitter and the receiver were made with a TRIMBLE GeoX7 and differentially corrected afterwards using the nearby correction station of Kumtor, resulting in a typical precision of 0.2 m.

75



80

**Figure 2:** Schematic setup of the measurements (upper panel) and example of a reflection signal used to infer the ice thickness (lower panel).

### 3.2. Yield stress method

85

Due to time and safety constraints, not all parts of the ice cap could be covered with measurements. Therefore, the yield stress method is employed to partly fill in the gaps (Figure 1). This method assumes perfect plasticity (Linsbauer et al., 2012; Li et al., 2012; Zekollari et al., 2013). The assumption is that the yield stress (basal shear stress) can be determined for measured points (Eq. 2) and that the mean yield stress can be assigned to unmeasured locations to infer the ice thickness along flowlines.

90

$$\tau_y = \rho g H \sin \alpha \quad (2)$$

$\alpha$  is the local surface slope averaged over a 250x250 m square and  $\rho$  is the average ice density (900 kg/m<sup>3</sup>).  $H$  is the local ice thickness. As the Grigoriev ice cap is not surrounded by valley walls, no shape factor to account for lateral drag is included here (Li et al., 2012; Pieczonka et al., 2018). However, since a large part of the ice cap was accessible for measurements, we opted not to assign the mean yield stress, but to interpolate the yield stress over the ice cap and assign the obtained value ( $\tau_y^*$ ) to the individual points at the position of the flowlines (Figure 1). Subsequently, the local ice thickness for the flowlines was inferred from Eq. 3:

100

$$H = \frac{\tau_y^*}{\rho g \sin \alpha} \quad (3)$$

Previous studies (Li et al., 2012; Farinotti et al., 2017) showed that Eq. 3 tends to overestimate the ice thickness in very flat regions (small slope). Therefore, we implemented a minimum slope of 5% and only determined the



105 ice thickness for points with larger slopes (Pieczonka et al., 2018). We also derived the mean yield stress, which  
appeared to be 73.3 kPa. This matches quite closely with the empirical based basal shear stress determined with  
the formula of Haeberli and Hoelzle (1995), which is equal to 78.88 kPa.

### 110 3.3. Anudem interpolation

In addition to all measurements and reconstructed flowline points, as boundary condition, the ice thickness  
along the margin of the ice cap was set to 5 m, which is a realistic assumption for grid points situated at 12.5 m  
from the margin ( $\sim$  half horizontal resolution) (Zekollari et al., 2013). However, the Grigoriev is also characterised  
by dry calving cliffs at the northern margin (Figure 1). Therefore, the ice thickness along this part was manually  
115 adjusted based on the elevation difference between the ice margin and the bedrock next to it. Finally, to achieve  
a full ice thickness distribution of the ice cap, all ice thickness data were interpolated to the entire ice cap using  
the Topo-To-Raster algorithm (Hutchinson, 1989; Fischer, 2009; Linsbauer et al., 2012; Van Tricht et al., 2021a).  
The resolution of the final ice thickness distribution was set to 25 m.

## 120 4. Results and discussion

### 4.1. Measured ice thickness and estimated volume

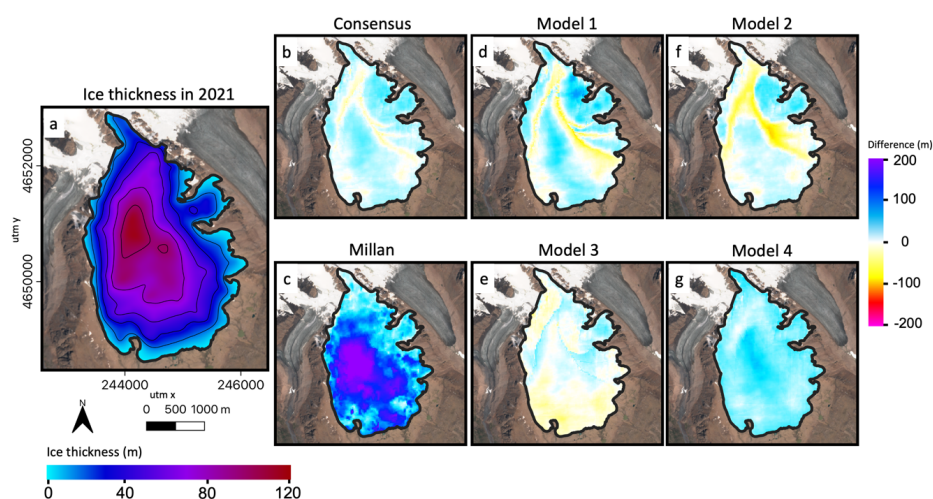
During the field campaign, the ice thickness was successfully determined for 481 locations. For ca. 30 locations,  
no clear ice thickness could be found because of distortions in the waveform. The mean measured ice thickness  
125 appeared to be  $73.05 \pm 11.65$  m, while the maximal measured ice thickness was  $114.85 \pm 13.74$  m. Takeuchi et  
al. (2014) found an ice thickness of 86.87 m for the ice core that was taken in 2007 near the summit of the  
Grigoriev ice cap. For the location of the ice core, we found a thickness of  $78.30 \pm 11.91$  m (difference of ca. -8  
m), which is within the error bounds. A potential cause for the difference could be thinning of the ice at the  
summit between 2007 and 2021. Additionally, the thinner ice at the summit in 2021 might be partly explained  
130 by the assumed constant velocity of the radar wave used to infer the ice thickness. Velocity was assumed to be  
constant at  $1.68 \times 10^8$  m/s, which is the travel velocity for pure ice. However, there is a layer of snow and firn at  
the top of the ice cap, which can lead to underestimations of the ice thickness when using this constant travel  
velocity. Another potential cause for the difference is related to a thinning of the ice at the summit between  
2007 and 2021. After interpolation of all the ice thickness data, a total ice volume of 0.392 (0.312 - 0.473) km<sup>3</sup>  
135 was derived (Figure 3a).

### 4.2. Comparison with global ice thickness and volume estimates

We compare our results with six existing ice thickness distributions and volume estimates composed without in-  
situ data (Figure 2). The five different ice thickness distributions presented in Farinotti et al. (2019) as well as the  
140 Millan dataset (Millan et al., 2022) were constructed using the SRTM DEM and the Randolph Glacier Inventory  
(RGI) v6.0 outline. They can thus be assumed to refer to the state of the ice cap in 2002. As such, we also  
reconstruct our ice thickness distribution for 2002 by correcting the surface elevation for the change between  
2002 and 2021. This is done by adding the difference between the 2021 DEM and the SRTM DEM to the ice  
thickness in constructed in 2021. To avoid errors outside of the 2021 geometry, only the 2021 glaciated area is  
145 considered for the comparison. We obtain a volume of 0.428 km<sup>3</sup> for 2002. In general, the consensus estimate  
of Farinotti et al. (2019) is slightly thicker with a volume of 0.523 km<sup>3</sup> (Figure 3b). However, in the RGI the  
different parts of the ice cap are separated into different parts, which leads to clearly visible boundary effects  
(Figure 3b,d,e,f). As the ice thickness of models 1-3 (Huss and Farinotti, 2012; Frey et al., 2014; Maussion et al.,  
150 2019), used for the consensus estimate, is forced to reach 0 m at the margin of the RGI parts, the ice thickness  
is underestimated for the boundaries located over the ice cap. Only for model 4 (Fürst et al., 2017), no boundary  
effects are visible (Figure 3g), but this model overestimates the ice thickness substantially. Although the



155 magnitude of ice thickness is generally well captured, using the consensus estimate to determine the bedrock  
of the Grigoriev ice cap would result in ridges. To solve for the boundary effects, Millan et al. (2022) designed a  
new method based on the surface ice flow velocity. Their approach is to infer the ice thickness from the observed  
surface velocity from satellite images. It is clearly visible, however, that the ice thickness of the Millan dataset is  
significantly larger than our reconstructed ice thickness field (Figure 3c). For the larger part of the ice cap, the  
Millan et al. (2022) estimate is between two to four times the measured ice thickness. For instance, the  
maximum ice thickness of the Millan dataset is 350 m, while we measured a maximum of  $114 \text{ m} \pm 13.74 \text{ m}$ .  
160 Regarding the volume, the Millan dataset has a volume of  $1.233 \text{ km}^3$  in 2001, which is 2.9x our reconstructed  
volume. The significantly thicker ice in the Millan dataset is related to an overestimation of the surface velocity.  
By comparing observed (from stakes) and modelled velocities with the velocities of Millan et al. (2022), we find  
a large discrepancy. For the thickest part, the Millan velocity map indicates velocities up to  $80 \text{ m yr}^{-1}$  while the  
stake and model derived velocities are in the order of  $3\text{-}5 \text{ m yr}^{-1}$  (Van Tricht and Huybrechts, 2022). We  
165 hypothesise that the velocities of this slowly moving ice cap have been substantially overestimated due to the  
presence of snow at the surface during most of the year, leading to low contrasts and an absence of features to  
trace over the year.



170 **Figure 3:** (a) Ice thickness of the Grigoriev ice cap in August 2021. Contours are added for every 20 m. The coordinate system  
corresponds to the EPSG:32644 WGS 84 / UTM zone 44N. (b-g) Difference between the created ice thickness distribution  
and the consensus estimate (Farinotti et al., 2019) (b), the different models used to compile the consensus estimate (d,e,f,g)  
and the Millan dataset (Millan et al., 2022) (c). The background of the seven panels is from Sentinel-2 in July 2021.

## 175 5. Conclusions

In this study, we measured and modelled the ice thickness of the Grigoriev ice cap in the Inner Tien Shan,  
Kyrgyzstan, and we compared the obtained ice thickness distribution with the results from 6 global ice thickness  
datasets. The main take-away from the analysis is that the consensus estimate of Farinotti et al. (2019) and the  
180 individual models from which it was composed, do not perform well enough yet for ice caps such as the Grigoriev  
ice cap. This is mainly caused by the division of the ice caps into multiple valley type glaciers and the dominance  
of valley glaciers in the calibration of the models. This is a weakness that was already mentioned earlier (Farinotti  
et al., 2017). The newest dataset of Millan et al. (2022) captures the ice thickness pattern well but grossly  
overestimates the ice thickness. Our results therefore show that local ice thickness measurements, especially  
185 on smaller or slow-flowing ice caps such as the Grigoriev ice cap, are still necessary for an accurate  
representation of ice thickness and resulting volume estimates.



## 6. Data availability

190 Research data and results are provided through an online public repository, accessible via  
191 <https://zenodo.org/badge/latestdoi/614248752> (Van Tricht, 2023). Information and specific details about the  
192 model code will be specified on request by Lander Van Tricht. The ice thickness measurements will be provided  
193 to the GlaThiDa (<https://www.gtn-g.ch/glathida/>).

## 7. Author contribution

195

All authors contributed to the fieldwork. LVT conducted the research and wrote the manuscript with help from  
PH and CMP. OR organised the fieldwork. We also specifically want to thank Benjamin Vanbiervliet, who assisted  
during the field campaign and helped to analyse preliminary data.

200

## 8. Competing interests

The authors declare that they have no conflict of interest.

## 9. Acknowledgements

205

We would like to thank everyone who contributed to the fieldwork.

## 10. Financial Support

210

Lander Van Tricht holds a PhD fellowship of the Research Foundation-Flanders (FWO-Vlaanderen) and is  
affiliated with the Vrije Universiteit Brussel (VUB).

## 11. References

215

Arkhypov, S.M., Mikhailenko, V.N., Kunakhovich, M.G., Dikikh, A.N. and Nagornov, O.V.: Termicheskiy rezhim,  
usloviya i doobrazovaniya i akumulatsiya na ladnike Grigor'eva (Tyan'-Shan') v 1962–2001 gg. [Thermal  
regime, ice types and accumulation in Grigoriev Glacier, Tien Shan, 1962–2001], *Materialy Glyatsiologicheskikh  
Issledovaniy (Data of Glaciological Studies)*, 96, 77–83, 2004 (in Russian with English summary).

220

Clarke, G.K., Berthier, E., Schoof, C.G. and Jarosch, A.H.: Neural networks applied to estimating subglacial  
topography and glacier volume. *Journal of Climate*, 22(8), 2146–2160, <https://doi.org/10.1175/2008JCLI2572.1>,  
2009

225

Dikikh, A.N.: Temperature regime of flat-top glaciers (using Grigoriev as an Example) – *Glyatsiol. Issledovaniya  
na Tyan-Shane, Frunze*, N. 11, 32–35, 1965 (in Russian).

230

Dyrgerov, M. B.: Glacier mass balance and regime: data of measurements and analysis, University of Colorado  
Institute of Arctic and Alpine Research Occasional Paper 55, Boulder,  
[http://instaar.colorado.edu/other/occ\\_papers.html](http://instaar.colorado.edu/other/occ_papers.html) (last access: 09 March 2023), 2002

Farinotti, D, Huss, M, Bauder, A, Funk, M. and Truffer, M: A method to estimate the ice volume and ice-  
thickness distribution of alpine glaciers. *Journal of Glaciology*, 55(191), 422–430,



<https://doi.org/10.3189/002214309788816759>, 2009

- 235 Farinotti, D., Brinkerhoff, D. J., Clarke, G. K. C., Fürst, J. J., Frey, H., Gantayat, P., Gillet-Chaulet, F., Girard, C., Huss, M., Leclercq, P. W., Linsbauer, A., Machguth, H., Martin, C., Maussion, F., Morlighem, M., Mosbeux, C., Pandit, A., Portmann, A., Rabatel, A., Ramsankaran, R., Reerink, T. J., Sanchez, O., Stenoft, P. A., Singh Kumari, S., van Pelt, W. J. J., Anderson, B., Benham, T., Binder, D., Dowdeswell, J. A., Fischer, A., Helfricht, K., Kutuzov, S., Lavrentiev, I., McNabb, R., Gudmundsson, G. H., Li, H., and Andreassen, L. M.: How accurate are estimates of glacier ice thickness? Results from ITMIX, the Ice Thickness Models Intercomparison eXperiment, *The Cryosphere*, 11, 949–970, <https://doi.org/10.5194/tc-11-949-2017>, 2017
- 240 Farinotti, D., Huss, M., Fürst, J. J., Landmann, J., Machguth, H., Maussion, F. and Pandit, A.: A consensus estimate for the ice thickness distribution of all glaciers on Earth. *Nature Geoscience*, 12(3), 168–173. <https://doi.org/10.1038/s41561-019-0300-3>, 2019
- 245 Fischer, A: Calculation of glacier volume from sparse ice-thickness data, applied to Schaufelferner, Austria. *Journal of Glaciology* 55(191), 453–460, <https://doi.org/10.3189/002214309788816740>, 2009
- Frey, H, Haerberli, W, Linsbauer, A, Huggel, C and Paul, F (2010) A multi-level strategy for anticipating future glacier lake formation and associated hazard potentials. *Natural Hazards Earth System Sciences* 10(2), 339–352. doi: 10.5194/nhess-10-339-2010
- 250 Frey, H., Machguth, H., Huss, M., Huggel, C., Bajracharya, S., Bolch, T., Kulkarni, A., Linsbauer, A., Salzmann, N. and Stoffel, M.: Estimating the volume of glaciers in the Himalayan–Karakoram region using different methods, *The Cryosphere*, 8, 2313–2333, <https://doi.org/10.5194/tc-8-2313-2014>, 2014
- 255 Fujita, K., Takeuchi, N., Nikitin, S. A., Surazakov, A. B., Okamoto, S., Aizen, V. B., and Kubota, J.: Favorable climatic regime for maintaining the present-day geometry of the Gregoriev Glacier, Inner Tien Shan, *The Cryosphere*, 5, 539–549, <https://doi.org/10.5194/tc-5-539-2011>, 2011
- 260 Fürst, J. J., Gillet-Chaulet, F., Benham, T. J., Dowdeswell, J. A., Grabiec, M., Navarro, F., Pettersson, R., Moholdt, G., Nuth, C., Sass, B., Aas, K., Fettweis, X., Lang, C., Seehaus, T., and Braun, M.: Application of a two-step approach for mapping ice thickness to various glacier types on Svalbard, *The Cryosphere*, 11, 2003–2032, <https://doi.org/10.5194/tc-11-2003-2017>, 2017
- 265 Haerberli, W. and Hoelzle, M: Application of inventory data for estimating characteristics of and regional climate-change effects on mountain glaciers: a pilot study with the European Alps. *Annals of Glaciology* 21, 206–212, <https://doi.org/10.3189/S0260305500015834>, 1995
- 270 Huss, M. and Farinotti, D.: Distributed ice thickness and volume of all glaciers around the globe. *Journal of Geophysical Research: Earth Surface* 117(F4), <https://doi.org/10.1029/2012JF002523>, 2012
- Hutchinson, MF: A new procedure for gridding elevation and stream line data with automatic removal of spurious pits. *Journal of Hydrology* 106(3–4), 211–232, [https://doi.org/10.1016/0022-1694\(89\)90073-5](https://doi.org/10.1016/0022-1694(89)90073-5), 1989
- 275 Linsbauer, A, Paul, F and Haerberli, W: Modeling glacier thickness distribution and bed topography over entire mountain ranges with GlabTop: application of a fast and robust approach. *Journal of Geophysical Research: Earth Surface* 117(F3), <https://doi.org/10.1029/2011JF002313>, 2012
- 280 Li, H, Ng, F, Li, Z, Qin, D and Cheng, G: An extended ‘perfect-plasticity’ method for estimating ice thickness along the flow line of mountain glaciers. *Journal of Geophysical Research: Earth Surface* 117(F1), <https://doi.org/10.1029/2011JF002104>, 2012
- Maussion, F., Butenko, A., Champollion, N., Dusch, M., Eis, J., Fourteau, K., Gregor, P., Jarosch, A. H., Landmann, J., Oesterle, F., Recinos, B., Rothenpieler, T., Vlug, A., Wild, C. T., and Marzeion, B.: The Open Global



- 285 Glacier Model (OGGM) v1.1, *Geosci. Model Dev.*, 12, 909–931, <https://doi.org/10.5194/gmd-12-909-2019>, 2019
- Mikhalechenko, V. N.: Osobennosti massoobmena lednikov ploskikh vershin vnutrennego Tyan'-Shanya [Peculiarities of the mass exchange of flat summit glaciers of interior Tyan'-Shan'], *Materialy Glytsiologicheskikh Issledovaniy (Data of Glaciological Studies)*, 65, 86–92, 1989 (in Russian)
- 290 Millan, R., Mougnot, J., Rabatel, A. and Morlighem M: Ice velocity and thickness of the world's glaciers. *Nature Geoscience*, 15, 124–129, <https://doi.org/10.1038/s41561-021-00885-z>, 2022
- Narod, B.B. and Clarke, G.K.C.: Miniature high-power impulse transmitter for radio-echo sounding. *Journal of Glaciology* 40(134), 190–194, <https://doi.org/10.3189/s002214300000397x>, 1994
- 295 Pieczonka, T, Bolch, T, Kröhnert, M, Peters, J and Liu, S: Glacier branch lines and glacier ice thickness estimation for debris-covered glaciers in the Central Tien Shan. *Journal of Glaciology* 64(247), 835–849, <https://doi.org/10.1017/jog.2018.75>, 2018
- 300 Takeuchi, N., Fujita, K., Aizen, V. B., Narama, C., Yokoyama, Y., Okamoto, S., Naoki, K., and Kubota, J.: The disappearance of glaciers in the Tien Shan Mountains in Central Asia at the end of Pleistocene, *Quaternary Science Revision*, 103, 26–33, <https://doi.org/10.1016/j.quascirev.2014.09.006>, 2014
- 305 Van Tricht, L., Huybrechts, P., Van Breedam, J., Fürst, J., Rybak, O., Satylkanov, R., Ermenbaiev B., Popovnin V., Neyns, R., Paice C.M. and Malz, P.: Measuring and inferring the ice thickness distribution of four glaciers in the Tien Shan, Kyrgyzstan. *Journal of Glaciology*, 67(262), 269–286. <https://doi.org/10.1017/jog.2020.104>, 2021a
- 310 Van Tricht L., Paice C.M., Rybak O., Satylkanov R., Popovnin V., Solomina O. and Huybrechts P.: Reconstruction of the Historical (1750–2020) Mass Balance of Bordu, Kara-Batkak and Sary-Tor Glaciers in the Inner Tien Shan, Kyrgyzstan. *Frontiers in Earth Science*, 9, <https://doi.org/10.3389/feart.2021.734802>, 2021b
- 315 Van Tricht, L., Huybrechts, P., Van Breedam, J., Vanhulle, A., Van Oost, K., and Zekollari, H.: Estimating surface mass balance patterns from unoccupied aerial vehicle measurements in the ablation area of the Morteratsch–Pers glacier complex (Switzerland), *The Cryosphere*, 15, 4445–4464, <https://doi.org/10.5194/tc-15-4445-2021>, 2021c
- 320 Van Tricht, L. and Huybrechts, P.: Thermal regime of the Grigoriev ice cap and the Sary-Tor glacier in the inner Tien Shan, Kyrgyzstan, *The Cryosphere*, 16, 4513–4535, <https://doi.org/10.5194/tc-16-4513-2022>, 2022
- 320 Zekollari, H., Huybrechts, P., Fürst, J. J., Rybak, O., and Eisen, O.: Calibration of a higher-order 3-D ice-flow model of the Morteratsch glacier complex, Engadin, Switzerland, *Annals of Glaciology*, 54, 343–351, <https://doi.org/10.3189/2013AoG63A434>, 2013
- 325 Welty, E., Zemp, M., Navarro, F., Huss, M., Fürst, J. J., Gärtner-Roer, I., Landmann, J., Machguth, H., Naegeli, K., Andreassen, L. M., Farinotti, D., Li, H., and GlaThiDa Contributors: Worldwide version-controlled database of glacier thickness observations, *Earth Syst. Sci. Data*, 12, 3039–3055, <https://doi.org/10.5194/essd-12-3039-2020>, 2020.